

## Accredited Vector Magnetometer Calibration Facility

*K. Pajunpää*<sup>1</sup>, *E. Klimovich*<sup>2</sup>, *V. Korepanov*<sup>2</sup>, *P. Posio*<sup>1</sup>, *H. Nevanlinna*<sup>1</sup>, *W. Schmidt*<sup>1</sup>,  
*M. Genzer*<sup>1</sup>, *A.-M. Harri*<sup>1</sup> and *A. Lourenço*<sup>3\*</sup>

<sup>1</sup> Finnish Meteorological Institute, Space Research, Finland

<sup>2</sup> Lviv Centre of Institute of Space Research, Ukraine

<sup>3</sup> LusoSpace, Aerospace Technology Lda, Portugal

\*(present address: Instituto Superior de Engenharia de Lisboa, Portugal)

(Received: September 2007; Accepted: November 2007)

### *Abstract*

*The paper describes the accredited magnetometer calibration facility of the Nurmijärvi Geophysical Observatory of the Finnish Meteorological Institute. The magnetometer calibration is part of the Magnetic Calibration and Test Laboratory of the observatory, which was accredited by the Finnish Accreditation Services (FINAS) in August 2007. The facility comprises a three-axes coil system installed in a non-magnetic building, temperature test system and an automatic control and measuring system. Both analog and digital outputs of magnetometers can be connected to the control electronics and the calibration procedure can be run fully automatic or with a predefined protocol. Accurate orientation with optical methods allows determination of the angles between magnetic and mechanical axes of the magnetometer. Experimental results of a calibration of a satellite magnetometer are included to demonstrate the calibration concept.*

*Key words: magnetometer calibration, accreditation, accredited laboratory, magnetic observatory*

### *1. Introduction*

Magnetometers are used in various applications from sea-bottoms to other planets of the solar system. Magnetic measurements are one of the key methods when studying the structure of the Sun and planets and the Sun-Earth interaction (*Acuña, 1974, Glassmeier et al., 2001*). Magnetometers carried by satellites either for studying the environment or for measuring the orientation of the satellite need a careful calibration not only for knowing the transformation coefficients and temperature effects but also to know the absolute orientations of the sensors with respect to a reference direction. Magnetic air borne mapping (*Korhonen et al., 2007*) and magnetotelluric soundings (*Korja, 2007*) are examples of other applications of three-component magnetometers.

In this paper we will describe the Nurmijärvi Magnetometer Calibration Facility (abbreviation NuMCF) and present a calibration of one satellite magnetometer of Luso-space, Lisbon Portugal. The NuMCF is part of the magnetic calibration and test labora-

tory (NuMCTL) of the Nurmijärvi observatory of the Finnish Meteorological Institute, comprising of magnetometer and sight compass calibrations, magnetic cleanliness measurements and compass swing base measurements at airfields. The laboratory was built at the observatory where quiet magnetic environment together with a special non-magnetic calibration room, make reliable measurements possible. A three-component coil system (see Fig. 1), following an article by *Allred and Scollar* (1967), was built at the observatory already in 1986. This coil system together with DC power sources and current meters was used manually until the middle of 1990's when an automatic control and measuring system was built for magnetometer calibrations (see Fig. 3). This modernizing was done in collaboration with Lviv Centre of Institute of Space Research in Ukraine (*Pajunpää et al.*, 1997). As a last stage of the development the Finnish Accreditation Service (FINAS) accredited in August 2007 the NuMCF together with compass calibrations and compass swing base measurements.

## 2. *The NuMCF coil system*

The three axes coil system is shown in Fig. 1 and consists of three sets of four square coils with side lengths from 1.6 to 2.2 meters. The frame is made of aluminum.

Two inner coils have 22 turns of 2 mm diameter copper wire and two outer coils have 42 turns of 1 mm wire. The coils are placed on a 70 x 70 cm<sup>2</sup> top of concrete coming up to the floor level of the calibration room. A pillar made of glass bricks and a marble plate on top of it is standing on the concrete basement. The pillar serves as a non-magnetic stable base for the tested instruments.

Theoretically, the *Allred and Scollar* (1967) coil system of this size can produce uniform fields with errors less than 0.001 % in a volume with diameter of about 30 cm at the centre of the system. A calculation based on real dimensions of the Nurmijärvi coil system, give 18 cm for the corresponding diameter for Y-component, 25 cm for X and 30 cm for Z.

The magnetic directions of the coil system were determined with a DI-fluxgate, a non-magnetic theodolite having a fluxgate sensor fastened to its telescope (*Kring-Lauridsen*, 1985). The X-axis of the coil system is aligned with the geographic North and its offset is about 0.5 arc minutes to West. The directions of the three orthogonal magnetic fields of the coil system were measured with the DI-fluxgate and the angles between the orthogonal fields were calculated. This measurement and calculation was done first in the centre of the coil system and then 15 cm to north, east, south and west and 18 cm above and below of the centre. The offsets of the angles from 90 ° are shown in arc minutes in Fig. 2. Tilting of the Z-coils north or east is less than 0.3 ' in the centre and less than 0.5 ' in all the measured points.

From the angle errors we can estimate that the artificial magnetic fields are orthogonal with accuracy better than half of a minute of arc in a sphere of 20 cm diameter in the centre of the coil system. In the close vicinity of the centre the errors are less than a third of a minute.

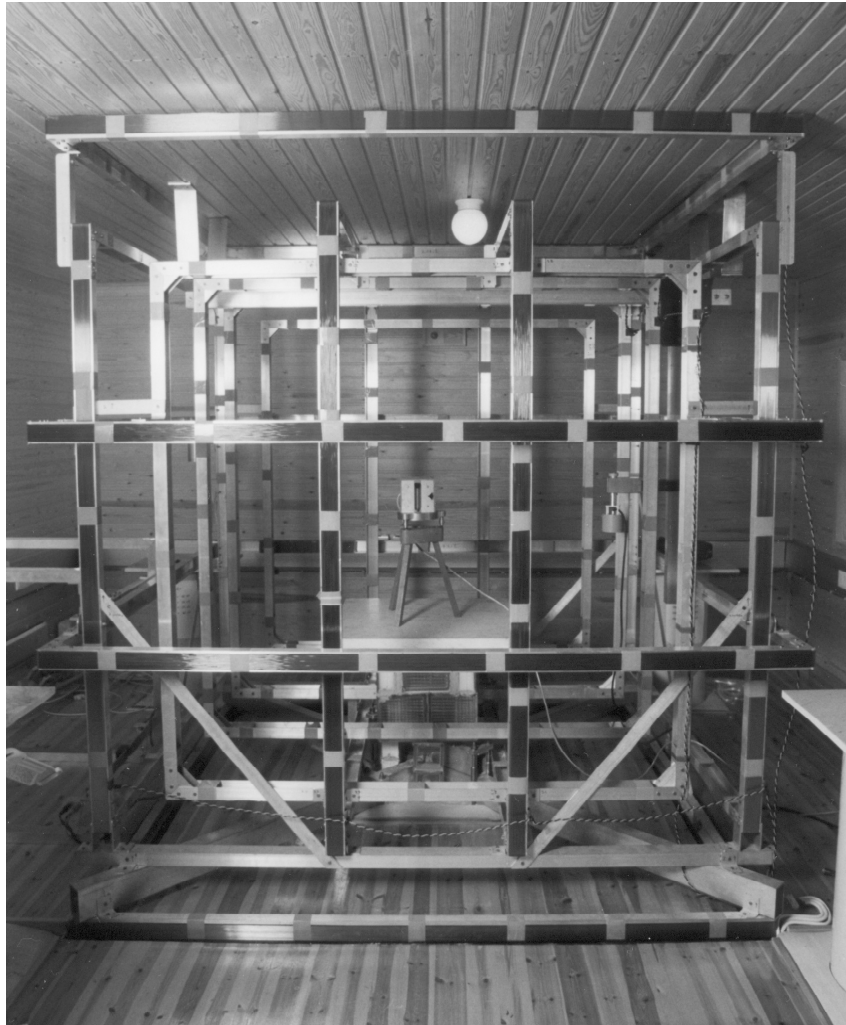


Fig. 1. Calibration coil system of the Nurmijärvi Geophysical Observatory.

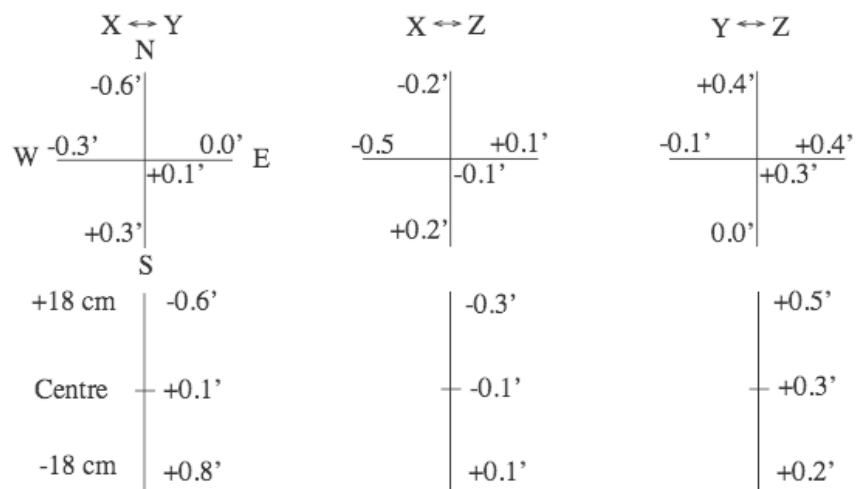


Fig. 2. Angle errors between the orthogonal magnetic fields in the centre of the coil system and 15 cm to north, east, south and west (above) and 18 cm above and below the centre (below).

The coil constants were measured by using a proton magnetometer in the centre of the coils. The Earth's field of two of the three components was first compensated to a value close to zero. Then large positive and negative fields were generated in the third component and the field in the centre of the coils was measured. With this method the coil constants can be measured with accuracy of  $\pm 0.002\%$ . This measurement is done once in every year and the values (Nov. 2006, 20 °C) were in [nT/mA]:  
X: 42.401, Y: 48.275 and Z: 36.970.

The coil dimensions depend on temperature and the coil constants have temperature dependencies of  $-0.0025\%/^{\circ}\text{C}$  for X component and  $-0.0020\%/^{\circ}\text{C}$  for Y and Z components.

### 3. *Operation principles of the NuMCF*

While the coil system is in the non-magnetic calibration room, the main part of the electronics of the NuMCF is installed on the basement of the observatory main building, some 30 meters from the calibration room, to avoid magnetic disturbances. The electronics consists of:

- Linux computer (PC) and local network for time and reference data
- Data collection DAQ (AT M10-16X-50) by National Instruments in the computer
- Three Kepco BOB-50-3 current sources
- Scaling amplifiers unit with 24-bit ADC
- Three precision reference resistors P321
- Preamplifier in the calibration room
- Thermal test electronics in the calibration room
- Computer in the calibration room.

#### 3.1 *Current measurement and control*

The regulation and measurement of current is fundamental for the accurate calibration. The precision resistors P321 are used as the reference elements for the current measurement. These resistors are first artificially then naturally aged during more than 20 years. The resistances of the reference resistors are corrected for the temperature to get the thermal stability of  $0.005\%/^{\circ}\text{C}$ .

The resistors are coupled in series with the coils (see Fig. 3). The voltage drops across the resistors are applied to the inputs of differential amplifiers located in the scaling amplifiers unit. The amplified voltage comes to the 24-bit ADC that transmits data through a RS232 interface to the PC.

The current values are defined either by the user (in a manual mode) or by the software (automatic mode) and the PC transmits to the DAQ the command to form voltages on the DAQ output. These voltages are used to control the KEPCO BOP amplifiers, which operate in current source mode and give the desired values of the currents to

the X, Y and Z coils. The current regulation process takes 6–7 seconds and the shortest measurement cycle of the system is 7–8 seconds. The resolution of the current control circuit corresponds to  $\pm 1$  nT in the magnetic field units. An arbitrary value of the field by each component can be created and kept within  $\pm 3$  nT in the working volume of the coils.

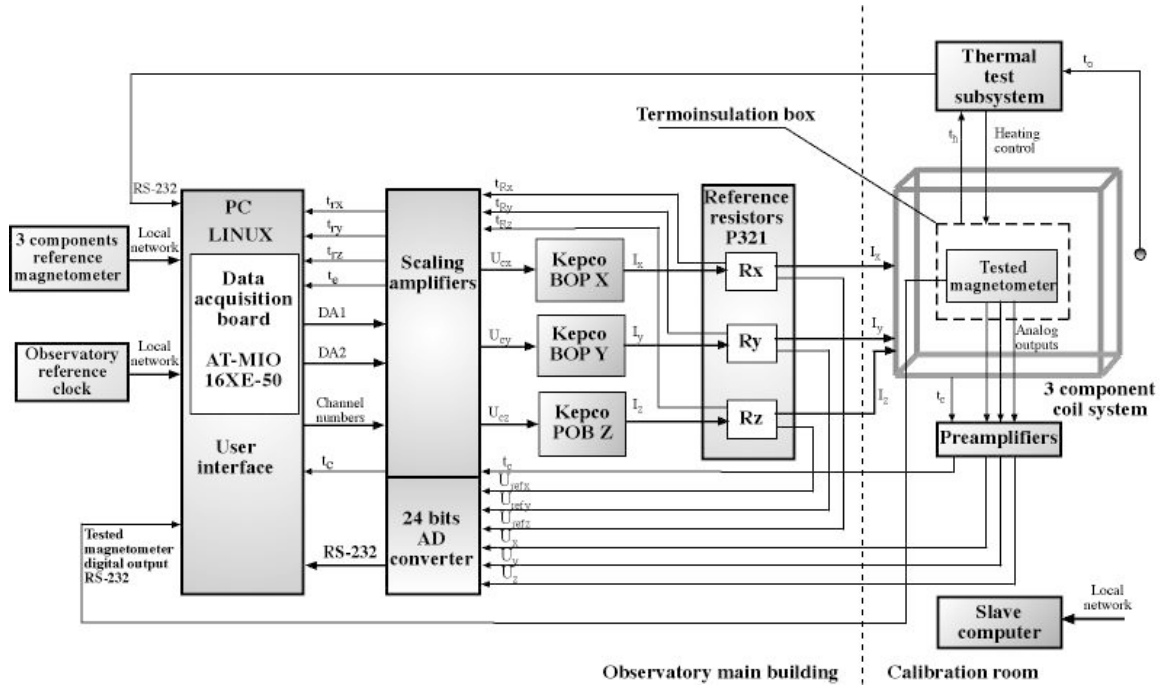


Fig. 3. Functional diagram of the magnetometer calibration system.

### 3.2 Tested magnetometer and reference magnetometer data

The NuMCF measures the voltages of the analog outputs of the tested magnetometer with the 24-bit ADC of the Scaling Amplifiers unit. Magnetometers with digital output can be connected to any computer in the network by using a prescribed exchange protocol. The calibration procedure is independent of the type of tested magnetometer connection.

Data from the three-component reference magnetometer come to the controlling PC through the local net. The reference magnetometer is a Danish suspended FGE (flux-gate) (*Rasmussen and Kring-Lauridsen, 1990*) in the temperature controlled variation house of the observatory, some 120 meters from the calibration coils. The data is used to correct for the Earth's magnetic field variations.

### 3.3 Optical sensor orientation

Often the exact knowledge of the orientations of the magnetometer sensor's magnetic axes with respect to the sensor's mechanical axes is needed. With this information the sensor can later be installed e.g. in a satellite so that the true magnetic directions of the magnetometer sensor are known with respect to reference directions of the satellite.

At NuMCF a theodolite can be installed on a pillar outdoors 60 m south from the coil system and along the magnetic South axis of the X-coils. By using a light beam from the theodolite (see Fig. 4) and a mirror fixed to the magnetometer sensor (in the centre of the coil system), the orientation of two mechanical axes of the sensor can be measured with accuracy better than  $\pm 0.03^\circ$ . The third axis is measured with a spirit level.

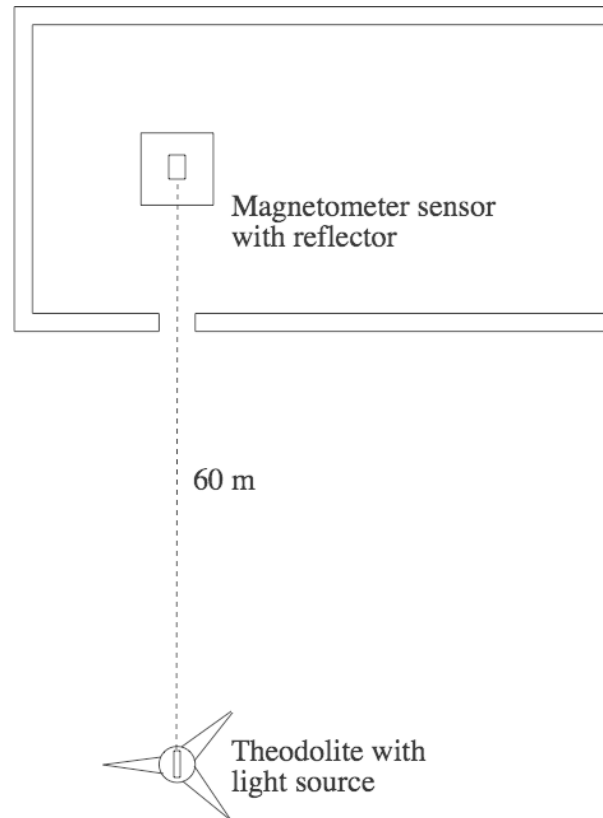


Fig. 4. Principle of the optical orientation of the magnetometer sensor in the calibration coil system. A top view of the magnetometer in the calibration house and the theodolite outdoors.

### 3.4 Thermal tests

The deformation and change of the material properties of a magnetometer sensor due to temperature variation can change the magnetic directions of the sensor, the transformation coefficients (the magnetic field at the sensor as input divided by the magnetometer output, nT/mV or nT/nT, for each component) and the offsets (the magnetometer output in zero field for each component). Therefore all these changes need to be determined especially for satellite magnetometers that may experience large temperature variations in space. The offset drift or in other words the base line drift is important e.g. for observatory magnetometers (*Csontos et al.*, 2007) and for magnetotelluric instruments.

The temperature variation is generated in a thermally insulated box (Fig. 5) that has a square hole in the bottom for a marble cube. The heating elements are fixed to the

marble and the tested magnetometer sensor is standing on the cube. The purpose of this arrangement is to avoid tilting of the underlain pillar due to heating or cooling. The box can be heated up to +60 °C and cooled by using dry ice down to about -30 °C.

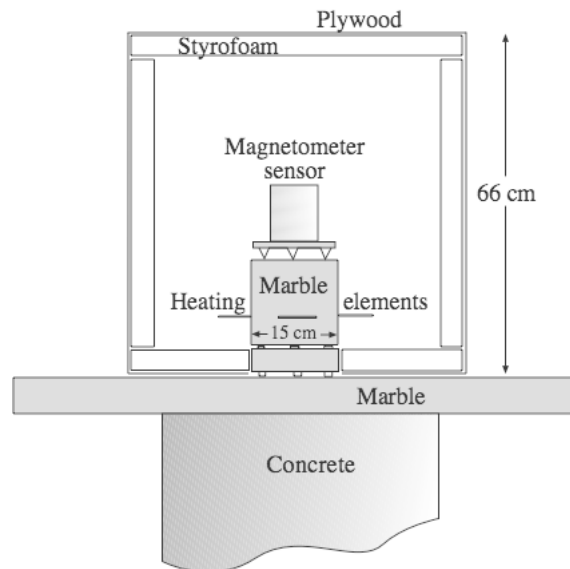


Fig. 5. Temperature test box with a tested magnetometer sensor.

The offset drift of the magnetometer is measured by recording the data of the tested magnetometer at various temperatures of the sensor or the electronics and by comparing the data with the data of the reference magnetometer (Danish suspended FGE). The transformation coefficients and the angles between the sensors can be measured in various temperatures. This is performed by transferring the box inside the coils and by heating or cooling the magnetometer sensor there in the center of the coil system.

### 3.5 User interface of the calibration software

The software of the calibration system was written in C language in Linux environment. The interactive user interface was made with Tcl/Tk. The following main menus are used:

- The Manual Control is used before automatic calibration to check the proper connection and orientation of the tested magnetometer.
- The Script File Control allows writing a predefined calibration procedure and running the predefined file.
- The Auto Control allows the software to choose for the calibration random field values within predefined limits or linear changes of the currents from minimal to maximal values or switching the current direction at every step. The random mode is the most common way of realizing the calibration.
- With the Thermal Test the thermal box is heated and the temperature drift of the magnetometer sensor or electronics is tested.

The procedures allow using unlimited number of measurements with different currents in the coils. Data from the coil currents, from the tested magnetometer output and from the reference magnetometer are stored in a file. The software calculates the calibration result already during the calibration and with all the data after it.

### 3.6 Calibration result

In the result of the calibration the following metrological parameters are determined:

- Transformation coefficients of the magnetometer's three components.
- Angles between the magnetic axes of the magnetometer.
- Angles between magnetic and mechanical axes of the magnetometer sensor.
- Temperature dependencies of transformation coefficients and of angles between magnetic axes of the sensor.
- Offset drifts of the magnetometer's three components due to temperature variation.
- Offsets of the magnetometer's three components.

The offset is determined in zero fields in the center of the coil system by simply measuring the tested magnetometer output in two reverse directions.

## 4. Accuracy considerations

### 4.1 Transformation coefficients

The estimation of the uncertainty of the measurements is based on the **EA-4/02** publication of the *EAL Committee 2* (1999) of the European co-operation for accreditation. The transformation coefficients  $T$  are obtained using Eq. (1) or (2) depending on the magnetometer output being analog or digital.

$$T_n = \frac{I_n * S_n}{U_n} \quad (1)$$

$$T_n = \frac{I_n * S_n}{B_{mag,n}} \quad (2)$$

where

$n$  = orthogonal components X, Y, Z

$I$  = current values fed into the coil system to generate artificial magnetic fields

$S$  = coil constants

$U$  = output voltage of the tested magnetometer

$B_{mag}$  = digital output of the tested magnetometer

Both U and I are measured with the same AD-converter. If the magnetometer output is digital, the divisor is a magnetic field value.

Temperature drift of the 1-ohm reference resistors is estimated to be the source of the largest error in the current measurement. With a measured maximum drift of 0.005 % over a +22 ... +32 °C temperature range and 80 mA (X), 70 mA (Y) and 90 mA (Z) as typical currents in a calibration, we get errors 0.004 mA, 0.0035 mA and 0.0045 mA. The standard uncertainty is computed assuming an U-shape distribution of the error:  $u(I_{TX}) = \pm 0.004/\sqrt{3}$  mA =  $\pm 0.0023$  mA,  $u(I_{TY}) = \pm 0.0020$  mA and  $u(I_{TZ}) = \pm 0.0026$  mA.

The current is measured by the AD-converter that covers the range  $\pm 2000$  mA of the X and Y components and  $\pm 3000$  mA of the Z-component. The experimental standard deviations due to the AD-converter error in the two ranges are 0.0028 mA and 0.0042 mA. By assuming 10 samples and a normal distribution of the error the standard uncertainties are  $u(I_{AD}) = \pm 0.0028/\sqrt{10}$  mA =  $\pm 0.0009$  mA for X and Y and  $\pm 0.0013$  mA for Z.

The combined standard uncertainties for the current measurement are calculated as square roots of the sums of the squared estimates of the two standard uncertainties above.

$$u(I_X) = \pm 0.0036 \text{ mA}$$

$$u(I_Y) = \pm 0.0034 \text{ mA}$$

$$u(I_Z) = \pm 0.0049 \text{ mA}$$

The coil constants are determined as a ratio of the total magnetic field measured with a proton magnetometer to the coil current measured with the calibration system. The standard uncertainty of the total field measurement is estimated to be  $\pm 0.2$  nT. Together with the standard uncertainty of the current measurement (the principle presented above) we get the standard uncertainties of the coil constants:

$$u(S_X) = \pm 0.00092 \text{ Nt/mA}$$

$$u(S_Y) = \pm 0.00099 \text{ Nt/mA}$$

$$u(S_Z) = \pm 0.00109 \text{ Nt/mA}$$

The output voltage of the tested magnetometer is measured with the AD-converter in the range  $\pm 10$  V. The experimental standard deviation (0.0045 %) of the voltage measurement gives for the standard uncertainty the value  $u(U) = \pm 0.06$  mV.

#### 4.1.1 *Experimental standard deviation of all observations*

The calibration result gives the standard deviation of the difference between the magnetic fields calculated from the currents in the coils and the fields calculated from the magnetometer outputs multiplied by the transformation coefficients and the angle correction matrix. The experimental variance in a simplified form is given in the Eq. (3) and the experimental standard deviation is  $s(B)$ .

$$s^2(B) = \frac{1}{m-1} \sum_{i=1}^m (B_{mag} - I * S)^2 \quad (3)$$

where

$B_{mag}$  = magnetometer output multiplied by the transformation coefficients and by the angle correction matrix.

$I$  = current value fed into the coil system to generate artificial magnetic fields.

$S$  = coil constant.

$m$  = number of successive measurements in the calibration.

We can calculate the experimental standard deviation of the mean as  $s(B_{ex}) = s(B)/\sqrt{m}$ .  $s(B)$  for a low noise magnetometer is usually of the order of 0.8 nT. A typical number of measurements  $m=25$  gives the standard uncertainty  $u(B_{ex}) = \pm 0.8/\sqrt{25}$  nT =  $\pm 0.16$  nT.

The experimental standard deviation  $s(B)$  increases with the increase of the noise of the tested magnetometer and with the field range used for the calibration. The field range can vary from small (e.g.  $\pm 100$  nT) up to the maximum of  $\pm 100000$  nT. Also the standard uncertainty of the current measurement is affected. Therefore the standard uncertainties  $u(B_{ex})$  and  $u(I)$  need to be determined case by case.

#### 4.1.2 Standard uncertainty of the transformation coefficients

The above components of the uncertainty were combined in an uncertainty budget to get the proper weight for every component. The budget in Table 1 for the X-component represents a usual calibration. The transformation coefficients are obtained from the partial derivatives of the function  $T = (I * S)/U$  with respect to  $I$ ,  $S$  and  $U$ . The transformation coefficient of  $B$  is calculated from the partial derivative of the ratio  $B/U$ .

Table 1. The uncertainty budget of the transformation coefficient of the X-component.

Quantity X-comp.	Estimate $x_i$	Standard uncertainty $u(x_i)$	Probability distribution	Sensitivity coefficient $c_i$	Contribution to stand. uncert. $u_i(y)$
I	80mA	0.0036mA	U-shape	0.0063nT/(mVmA)	0.000023nT/mV
S	42.40nT/mA	0.0009nT/mA	normal	0.012mA/mV	0.000011nT/mV
U	6784mV	0.06mV	normal	-0.00007nT/mV <sup>2</sup>	-0.000004nT/mV
B	3392nT	0.16nT	normal	0.00015 /mV	0.000024nT/mV
T	0.5nT/mV				$\pm 0.000035$ nT/mV $\pm 0.007$ %

Together with budgets for the other two components we get the standard uncertainties of the sensitivity coefficients:

$$u(T_X) = \pm 0.007\%$$

$$u(T_Y) = \pm 0.007\%$$

$$u(T_Z) = \pm 0.008\%$$

The **EA-4/02** publication for calibration laboratories states the use of an expanded uncertainty, obtained by multiplying the standard uncertainty  $u$  by the coverage factor  $k = 2$ . The assigned expanded uncertainty corresponds to a coverage probability of approximately 95 %. Here the multiplication with  $k = 2$  gives the expanded uncertainty of  $\pm 0.02\%$  for all the components.

#### 4.2 *Angles between the sensors*

Two input quantities affect the accuracy of the determination of the angles between the sensors:

D = errors in the magnetic directions of the coil system

C = accuracy of the determination of the angles from the measurement results

The magnetic directions of the orthogonal coil system are regularly measured with the DI-fluxgate instrument. Based on the measurements presented in the chapter 2 we can estimate that in the volume of 20 cm diameter around the center of the coil system the largest errors of the magnetic directions of the coils are less than  $\pm 30''$  and the standard uncertainty  $u(D) = 30''$ .

The deviation  $\alpha$  of the X-component of the magnetometer towards the Y-component of the coil system is calculated from the magnetic field generated in the X direction and the magnetic field measured by the Y-component of the magnetometer:  $\alpha = \arctan(Y/X)$ .

Assuming that the Y-component is 16 nT, the X-component 3392 nT we get  $\alpha = 0.27^\circ$ . The standard uncertainty of the of the magnetic field is  $\pm 0.16$  nT and the standard uncertainty of  $\alpha$  is

$$u(\alpha) = \frac{\sin(\alpha) * u(X) + \cos(\alpha) * u(Y)}{\sqrt{X^2 + Y^2}} \quad (4)$$

With the above numbers we get  $u(C) = u(\alpha) = 10''$ .

The contribution of the above two values  $u(D)$  and  $u(C)$  give to the standard uncertainty of the angular measurement the value  $\pm \sqrt{(u(D))^2 + (u(C))^2} = \pm 32''$ .

Multiplication with the coverage factor  $k = 2$  gives the expanded uncertainty of  $64''$  or  $0.02^\circ$

#### 4.3 *Angles between magnetic and mechanical axes of the magnetometer sensor*

The following parameters affect the accuracy of the optical orientation of the magnetometer sensor:

S = determination of the magnetic South direction of the coil system.

P = positioning of the theodolite along the magnetic South axis.

L = adjusting the magnetometer sensor so that the transmitted and reflected light beams unite at the theodolite outdoors.

The standard uncertainty of the direction measurement of the magnetic South of the coil system is estimated to be  $\pm 0.93''$ . Positioning of the theodolite outdoors can be done with better than  $\pm 0.5$  cm accuracy that corresponds to  $\pm 17''$  at the distance of 60 m. The light source can be brought within about 4 cm from the optical line of the theodolite. This means that the angle between the normal of the mirror plane and the optical axis of the theodolite is less than 1.1' (minutes of arc) or  $69''$ .

In the uncertainty budget the sensitivity coefficients for all these uncertainty estimates are 1 and the standard uncertainty of the optical orientation is  $41''$ . We take the standard uncertainty  $\pm 32''$  obtained in 4.2 as the error estimate for the determination of the magnetic axes of the magnetometer sensor. The value  $\pm \sqrt{(32^2 + 41^2)}'' = \pm 52''$  is then the standard uncertainty for the determination of the angle between magnetic and mechanical axes of the magnetometer sensor. We multiply the standard uncertainty by the coverage factor  $k = 2$  and get the value  $\pm 104''$  or 1.7' or  $0.03^\circ$ .

#### 4.4 *Offset determination*

The following parameters affect the accuracy of the offset measurement of the magnetometer sensor:

P = positioning of the sensor in the field with gradient.

D = orientation of the sensor in the opposite directions.

T = vertical tilting of the magnetometer sensor.

F = variations of the external field.

The errors of D and F are estimated to be zero due to repetition of the measurement in offset determination. The P and T may both have a systematic error and the standard uncertainty for both is  $\pm 0.29$  nT. An experiment of six offset determinations gave for the experimental standard deviation the value  $\pm 0.35$  nT and the standard uncertainty  $\pm 0.14$  nT.

The uncertainty budget gives  $\pm 0.43$  nT for the standard uncertainty of the offset determination.

Multiplying the standard uncertainty by the coverage factor  $k = 2$  and gives the value of  $\pm 1$  nT.

#### 4.5 Measurement capability

The combination of the results of the estimation of the expanded standard uncertainties of all the calibration results gives the measurement capability as in Table 2.

Table 2. Measurement capability and the expanded standard uncertainty of the NuMCF.

Magnetometer calibration Quantity	Temperature range	Expanded standard uncertainty ( $\pm$ )
Angles between the orthogonal components of magnetometer	-30 °C ... +60 °C	0.02 °
Angles between magnetic and mechanical axes of magnetometer		0.03 °
Transformation coefficients of magnetometer	-30 °C ... +60 °C	0.02 %
Offset of magnetometer		1 nT

#### 5. Accreditation of the NuMCF

In August 2007 the Finnish Accreditation Service (FINAS) accredited the NuMCF and the whole Nurmijärvi Magnetic Calibration and Test Laboratory. The accreditation was based on the decision K050/A01/2007 of FINAS and conforms to the requirements of the standard SFS-EN ISO/IEC 17025:2005 (*ISO/CASCO and CEN/CLC/TC 1, 2005*). The quality system for the NuMCTL was built in 2004-2006 and the application for accreditation was given to FINAS in October 2006.

The aim of the accreditation is to conform the traceability of the measured quantities to the international system of units (SI), and to ascertain that the measurements are performed in an acceptable way. The traceability concerns especially the magnetic flux density and the direction of the magnetic field that are also basic measurements of a magnetic observatory.

#### 6. NuMCF in service: Calibration of satellite magnetometer

A satellite AMR (Anisotropic MagnetoResistive) magnetometer of the Luso-Space, Aerospace Technology Lda in Lisbon, Portugal was calibrated in July 2005 at Nurmijärvi. The magnetometer was fixed on a base plate together with a mirror. The base plate was fixed on an Askania non-magnetic theodolite that can be rotated and leveled in a controlled manner. The analog output of the magnetometer was connected to the calibration system to carry out automatic calibration.

A series of calibrations were done, first round zero fields with 400 arbitrary field variations in the limits  $\pm 70000$  nT for X and Y components and  $\pm 60000$  nT for Z component. The Fig. 6 was generated by the calibration system and shows the Earth's magnetic field variations on the left and the difference between the magnetic fields calcu-

lated from the coil current and from the magnetometer output on the two other columns. In the middle the difference is a function of the number of observation (or time) and on the right a function of the magnetic field generated by the coil system.

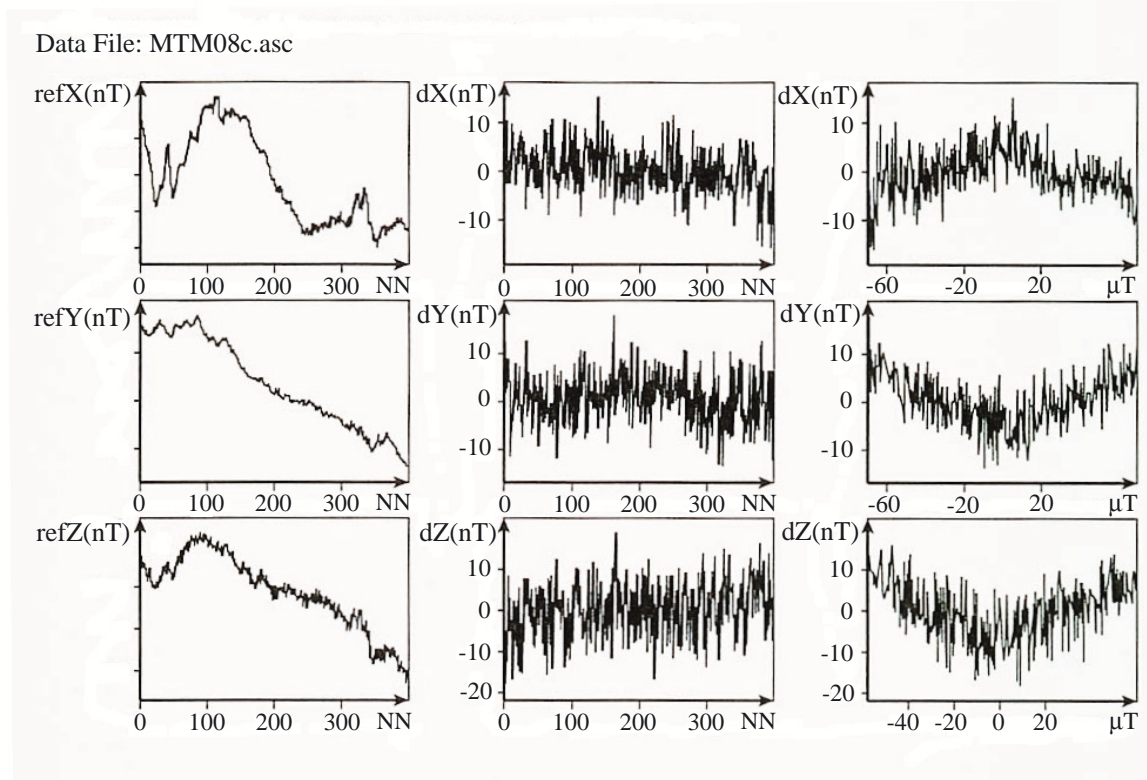


Fig. 6. Graphics window during the calibration. The rows represent the components X, Y and Z. The first column shows the Earth's field variation. The second and third columns give the difference between the fields calculated from the coil current and from the tested magnetometer output. The horizontal axis of the first and second columns is the number of measurements (time) and the horizontal axis of the third column is the total magnetic field in the centre of the coils.

The right column gives an estimate of the non-linear behavior of the magnetometer. For an optimal magnetometer the difference values of the third column would draw straight horizontal lines. Here we can estimate that the linearity error is less than  $\pm 0.025\%$  for all the components. The peak-to-peak noise of the differences in the right column is about 20 nT that is due to the large field variations used in this test and due to the noise of the magnetometer. (The absolute error of the current measurement increases with the increasing amplitude of the current. With small variations e.g.  $\pm 2000$  nT and a low noise magnetometer the peak-to-peak noise is usually less than 2 nT.)

The calibration software used all the 400 three-component electric current values, reference magnetometer observations and the voltage outputs of the tested magnetometer and calculated the angles between the magnetic directions of the sensor and the transformation coefficients. The standard deviations were calculated of the differences between the magnetic fields calculated from the coil currents and from the tested magnetometer output. The results are presented in Table 3.

Table 3. Angles between the magnetic axes of the magnetometer sensor [degrees], transformation coefficients  $S$  of the three components and standard deviations  $Std$  of the differences between the magnetic fields calculated from the coil currents and from the tested magnetometer output.

$X \Leftrightarrow Y$	$Y \Leftrightarrow Z$	$X \Leftrightarrow Z$
88.83 °	88.64 °	88.26 °
$S_x$ [nT/mV]	$S_y$ [nT/mV]	$S_z$ [nT/mV]
15.365	15.172	14.814
$Std_x$ [nT]	$Std_y$ [nT]	$Std_z$ [nT]
5.7	6.2	8.2

Next the angles between magnetic and mechanical axes of the magnetometer were determined. A theodolite was installed on the pillar at 60 m distance from the magnetometer and along the magnetic South axis of the coil system. The magnetometer sensor together with the mirror was turned so that the light beam from the theodolite returned back to the theodolite. The Y-axis normal to the light beam was leveled with a spirit level. An altitude difference of few centimeters was corrected in the calculation. The sensor of the tested magnetometer was directed as X to the North, Y to the West and Z up. The results are presented in Table 4 together with offsets. The offsets of the magnetometer were measured in zero fields (<20 nT) by observing the field several times at two opposite directions.

Table 4. Angles between the magnetic axes and the mechanical axes of the magnetometer sensor and offsets of the magnetometer.

X-sensor North $\Rightarrow$ West	Y-sensor West $\Rightarrow$ South	Z-sensor Up $\Rightarrow$ North
1.43 °	0.27 °	2.98 °
X-Y plane $\Rightarrow$ Up	X-Y plane $\Rightarrow$ Up	X-Z plane $\Rightarrow$ West
0.75 °	0.60 °	0.77 °
$Off_x$ [nT]	$Off_y$ [nT]	$Off_z$ [nT]
-17	-16	+35

In the last test the magnetometer was cooled and heated to get the temperature variation of the transformation coefficients and of the angles between the magnetic directions of the sensor. The temperature test box was installed in the calibration coil system so that the sensors were again in the middle of the coils. The box was heated with the software controlled heating system. The cold temperature (-10 °C) was made with dry ice after keeping the magnetometer two hours in a deep freeze (-18 °C). The temperature during the test was measured inside the magnetometer with its own sensor. The Fig. 7 and Fig. 8 show the results of the test.

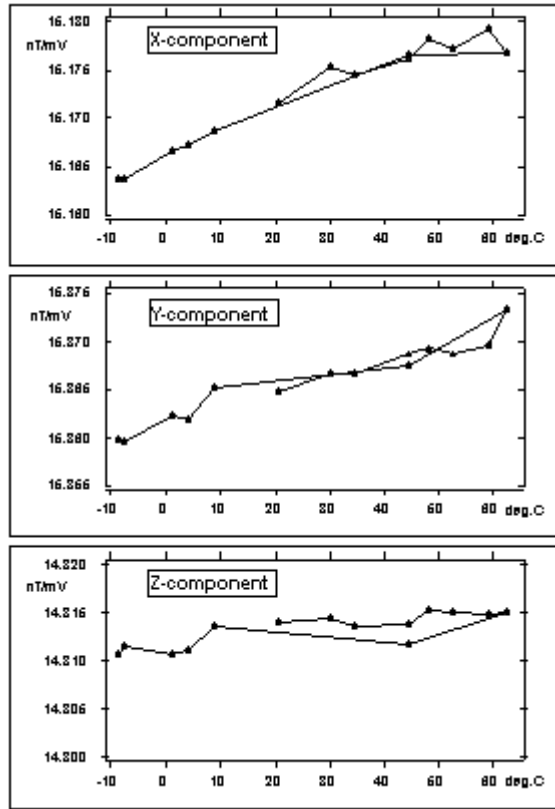


Fig. 7. The transformation coefficients of the magnetometer as a function of temperature.

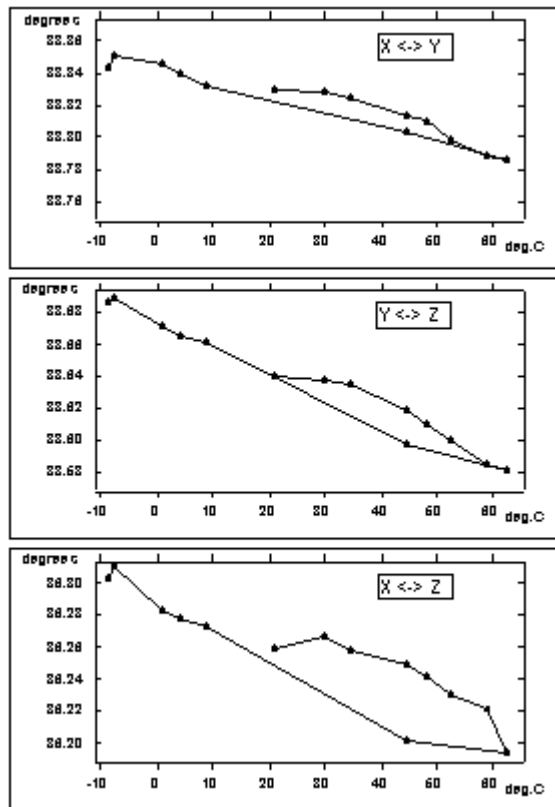


Fig. 8. The angles between the sensors as a function of temperature.

The expanded uncertainty of measurement was reported as the standard uncertainty multiplied by the coverage factor  $k = 2$ . This corresponds to a coverage probability of approximately 95 %.

Angles between the sensors:	$\pm 0.02^\circ$
Deviations of the sensors from the reference directions:	$\pm 0.05^\circ$
Transformation coefficients:	$\pm 0.03\%$
Offsets of the sensors:	$\pm 2\text{ nT}$

## 7. *Concluding remarks and discussion*

The Nurmijärvi Magnetic Calibration Facility provides equipment and means for accurate calibration of three-component magnetometers both for satellite and ground based observations. The calibration procedures include determination of transformation coefficients and angles between the magnetic directions of the tested magnetometer at different temperatures, directions of the magnetic axes with respect to the mechanical axes of the magnetometer, offsets and temperature drifts. Analog or digital output of the tested magnetometer can be connected to the calibration system to enable fast and automatic calibration. The angles between magnetic and mechanical axes are measured with help of optical orientation of the sensor. Temperature variations are generated in a special thermal testing box.

A practical example of the service of the NuMCF is presented as the calibration of the satellite magnetometer of the LusoSpace, Aerospace Technology Lda Lisbon. The base plate of the magnetometer sensor was furnished with a mirror and with a light beam the mirror normal was accurately directed to the South axis of the coil system. Thereafter the angles between magnetic axes of the magnetometer and the mechanical axes determined with the mirror and the base plate were measured. The temperature dependences of the transformation coefficients and of the angles of the magnetic axes of the magnetometer were measured in the temperature range  $-10 \dots +60^\circ\text{C}$ . The measured parameters were presented and their accuracies were estimated.

The NuMCF is one of the most advanced magnetometer calibration facilities in the whole World. A quality system for the NuMCTL was built during 2004-2006 and the NuMCF as part of the laboratory was accredited by FINAS in August 2007.

A calibration system similar to the NuMCF was delivered to the Canberra magnetic observatory of the Australian Geological Survey in 1999. The equipment and method can be subject for another construction in another part of the World.

## 8. *Acknowledgements*

The authors wish to thank two anonymous referees for their patience in reading the manuscript and making numerous constructive comments.

*References*

- Acuña, M., 1974. Fluxgate magnetometers for outer planet exploration, *IEEE Transactions on Magnetics*, **10** issue 3, 519–523.
- Allred, J.C. and I. Scollar, 1967. Square cross section coils for the production of uniform magnetic fields, *J. Sci. Instrum.*, **44**, 755–760.
- Csontos, A., L. Hegymegi and B. Heilig, 2007. Temperature tests on modern magnetometers, *Proceedings of the XII IAGA Workshop on Geomagnetic Observatory Instruments, Data Acquisition and Processing, Belsk 19–24 June 2006*, 171–177.
- EAL Committee 2, 1999. EA-4/02 - Expression of the Uncertainty of Measurement in Calibration, 79 pp.
- Glassmeier, K.-H., U. Motschmann, M. Dunlop, A. Balogh, M.H. Acuña, C. Carr, G. Musmann, K.-H. Fornacon, K. Schweda, J. Vogt, E. Georgescu and S. Buchert, 2001. Cluster as a wave telescope – first results from the fluxgate magnetometer, *Annales Geophysicae*, **19**, Issue 10, pp.1439–1447.
- ISO/CASCO and CEN/CLC/TC 1, 2005. General requirements for the competence of testing and calibration laboratories (SFS-EN ISO/IEC 17025:2005), *Finnish Standards Association*, 61 pp.
- Korhonen, J.V., J.D. Fairhead, M. Hamoudi, K. Hemant, V. Lesur, M. Manda, S. Maus, M. Purucker, D. Ravat, T. Sazonova and E. Thébaud, 2007. Magnetic anomaly map of the world = Carte des anomalies magnétiques du monde. Scale = Echelle 1:50,000,000. Paris: CCGM - CGMW.
- Korja, T., 2007. How is the European lithosphere imaged by magnetotellurics? *Surv. Geophys.*, **28**, 239–272.
- Kring-Lauridsen, E., 1985. Experience with the DI-fluxgate magnetometer inclusive theory of the instrument and comparison with other methods, *Geophysical Papers R-71, Danish Meteorological Institute, Copenhagen*, 30 pp.
- Pajunpää, K., V. Korepanov and E. Klimovich, 1997. Calibration system for vector DC magnetometers, *Proceedings of the XIV IMEKO World Congress, 1-6 June, 1997, Tampere, Finland.*, **IVA**, 97–102.
- Rasmussen, O. and E. Kring-Lauridsen, 1990. Improving baseline drift in fluxgate magnetometers caused by foundation movements, using suspended fluxgate sensor, *Phys. Earth Planet. Int.*, **59**, 78–81.